

# RRP Nb<sub>3</sub>Sn Strand Studies for LARP

Emanuela Barzi, Rodger Bossert, Shlomo Caspi, Daniel R. Dietderich, Paolo Ferracin, Arup Ghosh, Daniele Turrioni

**Abstract**— The Nb<sub>3</sub>Sn strand chosen for the next step in the magnet R&D of the U.S. LHC Accelerator Research Program is the 54/61 sub-element Restacked Rod Process by Oxford Instruments, Superconducting Technology. To ensure that the 0.7 mm RRP strands to be used in the upcoming LARP magnets are suitable, extensive studies were performed. Measurements included the critical current,  $I_c$ , using the voltage-current ( $V$ - $I$ ) method, the stability current,  $I_S$ , as the minimal quench current obtained with the voltage-field ( $V$ - $H$ ) method, and RRR. Magnetization was measured at low and high fields to determine the effective filament size and to detect flux jumps. Effects of heat treatment temperature and durations on  $I_c$  and  $I_S$  were also studied. Using strand billet qualification and tests of strands extracted from cables, the short sample limits of magnet performance were obtained. The details and the results of this investigation are herein described.

**Index Terms**— Nb<sub>3</sub>Sn, Restack Rod Process, critical current density, magnetic instability.

## I. INTRODUCTION

LARP Technology Quadrupoles (TQ) [1,2] and all other LHC Accelerator Research Program (LARP) magnet designs [3,4] are presently based on 0.7 mm Nb<sub>3</sub>Sn strands. The workhorse material chosen for the next step in the magnet R&D is the 54/61 subelement (*i.e.* 54 subelements in a 61-stack billet) Restacked Rod Process (RRP) by Oxford Instruments, Superconducting Technology (OIST). Meanwhile, the Conductor Development Program (CDP) and Fermilab [5] are working with designs with larger number of restacks to reduce the effective filament diameter,  $d_{eff}$ , which is known to play a substantial role in magnetic instabilities.

Strand studies start by checking that the billets being produced meet specifications. Extensive heat treatment (HT) optimization studies are then performed to meet the two conflicting requests of large critical current,  $I_c$ , at high field, and good stability at low fields. After cable fabrication, both high field  $I_c$  degradation and low field stability are studied and measured for all cables. Using witness (*i.e.* sample reacted with the coils) strand and cable samples, short sample limit

predictions are calculated for each coil that is wound and heat treated from measurements of extracted strands.

## II. STRAND AND CABLE SPECIFICATIONS

Based on feedback from previous R&D work [6], strand and cable specifications were formulated for the next LARP quadrupole models, as shown in Tables I and II. A description of the many cables fabricated within the LARP program is in [7].

TABLE I  
STRAND SPECIFICATIONS

| Technology                       | Ternary RRP Nb <sub>3</sub> Sn |
|----------------------------------|--------------------------------|
| Diameter, mm                     | 0.7                            |
| $J_c(12\ T)$ , A/mm <sup>2</sup> | ≥ 2400                         |
| $d_{eff}$ , μm                   | < 70                           |
| $I_S$ , A                        | > 1000                         |
| Cu, %                            | 53 ± 2                         |
| RRR                              | ≥ 100                          |
| RH twist, mm                     | 14 ± 2                         |
| Piece length, m                  | ≥ 350                          |
| High temperature HT time, hr     | ≥ 48                           |

TABLE II  
TQ CABLE SPECIFICATIONS

| Parameter           | Specification | Tolerance      |
|---------------------|---------------|----------------|
| No. strands         | 27            | -              |
| Strand diameter, mm | 0.7           | ± 0.002        |
| Width, mm           | 10.077 max    | +0.000, -0.100 |
| Thickness, mm       | 1.26          | ± 0.01         |
| Keystone angle, °   | 1             | ± 0.10         |
| Pitch length, mm    | 78            | ± 2            |
| Length, m           | 65            | -              |

## III. REACTION AND STRAND TEST PROCEDURES

### A. Reaction and Strand Test Procedures

The strand samples were mounted on grooved cylindrical barrels made of either Ti-6Al-4V (FNAL, LBNL) or stainless steel (BNL). After reaction in vacuum (BNL) or in Argon (FNAL, LBNL), the samples were either tested on the same barrel (FNAL, LBNL) or transferred to a Ti-alloy barrel (BNL) [6]. Unless otherwise specified, BNL used end splices soldered in parallel to a couple of sample end turns in the region of transition from the Cu to the Ti-alloy section of the barrel, and no bonding agent, and FNAL and LBNL used end splices and STYCAST to bond the sample. The  $I_c$  was determined from the  $V$ - $I$  curve using the 10<sup>-14</sup> Ω·m resistivity criterion. In  $V$ - $H$  tests the transport current is ramped to a fixed value, and the field is swept up and down between 0 and

Manuscript received August 28, 2006. This work was supported by the U.S. Department of Energy.

E. Barzi, R. Bossert and D. Turrioni are with the Fermi National Accelerator Laboratory, Batavia, IL 60510 USA (E. Barzi phone: 630-840-3446; fax: 630-840-3369; e-mail: [barzi@fnal.gov](mailto:barzi@fnal.gov)).

A. Ghosh is with the Brookhaven National Laboratory, Upton, NY 11973 USA.

S. Caspi, D. R. Dietderich and P. Ferracin are with the Lawrence Berkeley National Laboratory, Berkeley, CA 94720 USA.

4 T with ramp rates of 5 to 17 mT/s. If no quench is observed the current is increased and the test repeated. This test is done to determine the minimum quench current, or stability current,  $I_S$ , in the presence of a magnetic field variation. For strands, the  $I_S$  value was reported as the average between the minimal current at which a quench occurred and the maximum current that the sample could sustain without quenching.

Magnetization measurements at FNAL were conducted with a balanced coil magnetometer at low and high fields.

### B. Comparison of Test Results (Round Robin)

The reaction of SRS01, which is made of two double-layer racetrack coils, SRS01-C01 and SRS01-C02, was used also as a round robin test run among the Labs. These two coils underwent separate reactions at BNL. In each case strand and cable samples were included together with the coils to serve as witnesses of the coil reaction. Table III shows the test results obtained for extracted strands tested on Ti-alloy barrels. The difference in  $I_c$  test results between BNL and FNAL was 6% to 9% at 11 T.

TABLE III  
ROUND ROBIN TEST RESULTS

| SRS01-C01 Reaction |                  |                   |       |       |      |        |           |     |
|--------------------|------------------|-------------------|-------|-------|------|--------|-----------|-----|
| Strand ID          | $I_c, A$ at 15 T | 12 T <sup>a</sup> | 11 T  | 10 T  | 9 T  | 8 T    | $I_S, A$  | RRR |
| Extr. 935R, BNL    | [577]            | 706               | 859   | 1038  | -    | -      | 575±25    | 183 |
| Extr. 935R, BNL    | [557]            | 682               | 827   | 1001  | 1203 | -      | >1200     | 225 |
| Extr. 935R, FNAL   | 243              | 517               | [639] | (793) | -    | -      | 1287±12.5 | -   |
| SRS01-C02 Reaction |                  |                   |       |       |      |        |           |     |
| Strand ID          | $I_c, A$ at 15 T | 12 T <sup>a</sup> | 11 T  | 10 T  | 9 T  | 8 T    | $I_S, A$  | RRR |
| Extr. 935R, BNL    | [544]            | 667               | 812   | 983   | -    | -      | 950±50    | 176 |
| Extr. 935R, BNL    | [566]            | 694               | 838   | 1011  | 1216 | -      | 1050±50   | 174 |
| Extr. 935R, BNL    | [564]            | 684               | 841   | 1010  | 1225 | -      | >1200     | 355 |
| Extr. 935R, FNAL   | 245              | 525               | (646) | (796) | -    | (1157) | 975±25    | 297 |

<sup>a</sup> Values in square parentheses were parameterized using [8], values in round parentheses were extrapolated from the  $V-I$  curve.

### IV. BILLET PRODUCTION

OIST has presently produced for LARP eight billets for a total of about 280 kg of 0.7 mm RRP strand with 54/61 subelement design. Fig. 1 shows a strand cross section. The piece length distribution is shown in Fig. 2. Except from the first billet (8220) that was produced with a larger twist pitch, the right-hand pitch was  $13.4 \text{ mm} \pm 1.4 \text{ mm}$ , and the  $\text{Cu}\%$  was  $46.5 \pm 0.5$ . For a HT with a final step of 50 h at 665 °C, the RRR was  $187 \pm 32$ , and the average  $J_c(4.2 \text{ K}, 12 \text{ T})$  as measured by OIST at the front and back end of each billet was  $2891 \text{ A/mm}^2$  with a standard deviation of  $152 \text{ A/mm}^2$ .

Magnetization as measured at 4.2 K and 1.8 K at FNAL for a sample of billet 8817 is given in Fig. 3. The final HT step was 60 h at 635 °C. Magnetization  $\mu_0 M(4.2 \text{ K}, 12 \text{ T})$  per total strand volume was  $(55.4 \pm 1.8) \text{ mT}$ . The  $I_c(4.2 \text{ K}, 12 \text{ T})$  was 532 A. The resulting  $d_{\text{eff}}$  in the round filament approximation was  $(78.7 \pm 2.6) \mu\text{m}$ . At 1.8 K,  $\mu_0 M(1.8 \text{ K}, 12 \text{ T})$  per total strand volume was  $(75.1 \pm 3.9) \text{ mT}$ , which indicates that the  $I_c(1.8 \text{ K}, 12 \text{ T})$  is a factor of 1.35 larger than  $I_c(4.2 \text{ K}, 12 \text{ T})$ . However, at low field flux jumps at 1.8 K are so large that they reduce the magnetization amplitude by about 30% compared to data

at 4.2 K. More magnetization test results on LARP strands can be found in [9].

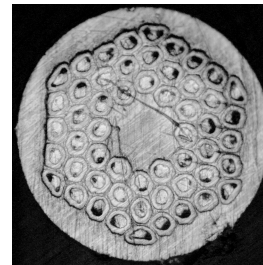


Fig. 1. Cross section of a reacted 0.7 mm RRP strand.

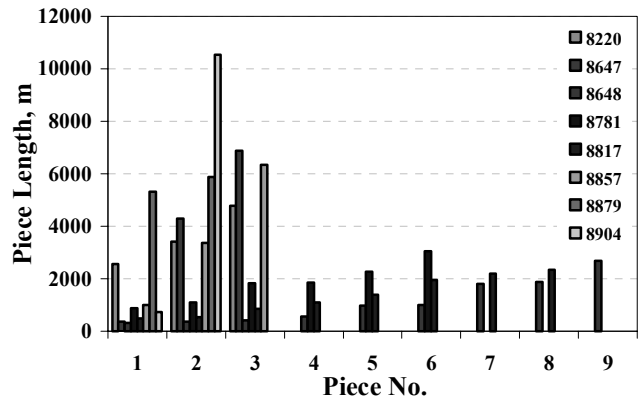


Fig. 2. Distribution of piece lengths for the OIST billets.

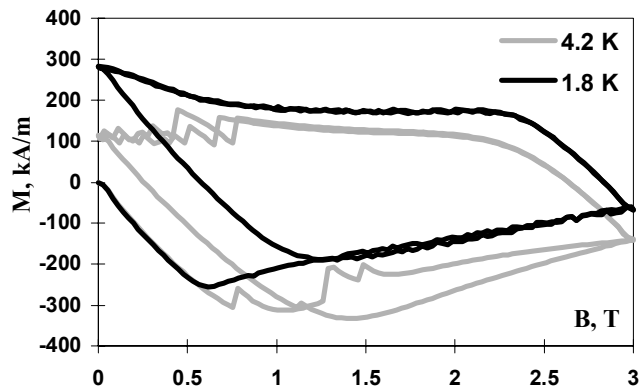


Fig. 3. Magnetization curves per total volume of an 8817 RRP strand at low field at 4.2 K and at 1.8 K.

### V. OPTIMIZATION OF REACTION CYCLE

To establish a suitable heat treatment schedule for the first RRP TQ and SR magnets, heat treatment optimization cycles that provide good  $I_c$  and  $I_S$  were searched. Three billets, 8220, 8647 and 8648, were used for this study. The  $I_c(11 \text{ T})$  and the  $I_S$  as measured at 4.2 K for round strands at BNL are plotted in Figs. 4 and 5 as a function of maximum reaction temperature. The duration was 48 to 50 h in all cases. The spread in data associated to a same temperature is a measure of the reproducibility that can be attained in  $I_c$  and  $I_S$  tests. One can see that whereas the largest  $I_c$  are obtained at temperatures between 660 °C and 680 °C, the largest  $I_S$  are found below

660 °C.

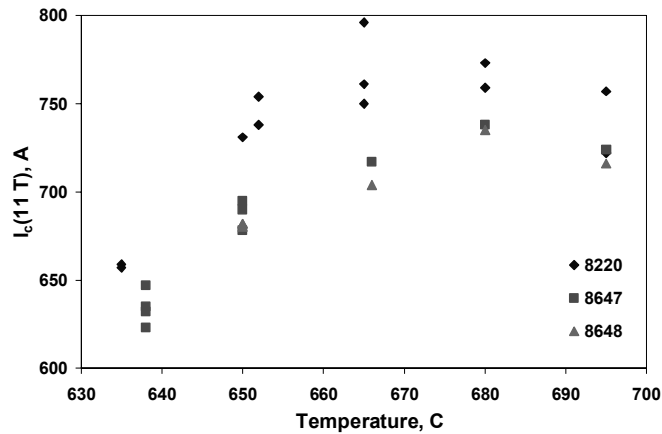


Fig. 4.  $I_c(11 T)$  as measured at 4.2 K at BNL for round strands of three billets as a function of reaction temperature for 48 to 50 h durations.

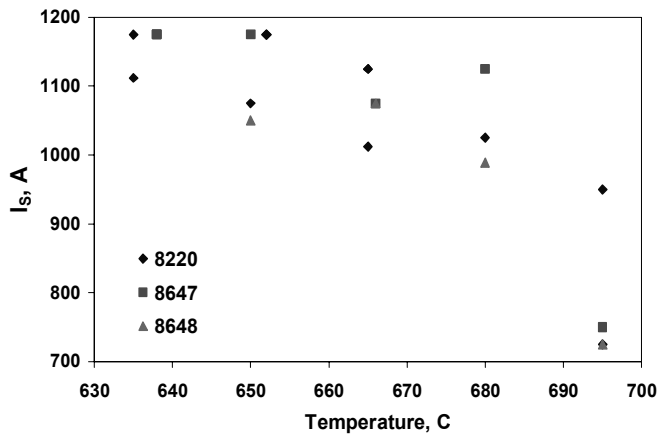


Fig. 5.  $I_S$  as measured at 4.2 K at BNL for round strands of three billets as a function of reaction temperature for 48 to 50 h durations.

## VI. CABLE QUALIFICATION

An example of cable qualification is given for three different cables that were all made out of the same billet 8220. Cables 933R and 939R meet TQ cable specs, cable 935 is a narrower rectangular cable made of 20 strands, to be used in the small and long racetracks [7].

### A. High Field $I_c$ Degradation

For these three cables, the  $I_c(11 T)$  as measured at 4.2 K at BNL for extracted strands is given as a function of reaction temperature for 48 to 50 h durations in Fig. 6. Results are compared against round strand data. One can see that  $I_c$  degradation is usually contained, albeit not always reproducible. For instance in the case of cable 939R, which was deemed damaged after microscopic evaluation [7], the maximum  $I_c$  degradation ranged between 3% and 8%, which is very similar to that of cable 935R, which was of ~5%. Cable 935R was not deemed damaged after microscopic analysis.

### B. Low Field Stability

The  $I_S$  as measured at 4.2 K at BNL for strands extracted from the three cables is given as a function of reaction

temperature for 48 to 50 h durations in Fig. 7. Results are compared against round strand data. The  $RRR$  values obtained as the ratio of  $R(295 K)$  and  $R(18 K)$  for 20 cm long samples are shown in Fig. 8. The  $I_S$  and  $RRR$  values of extracted strands usually lie beneath the upper envelope defined by round strand data, and are not as reproducible as in round strands as the spread in results associated to a same temperature is usually larger for extracted strands, at least up to 680 °C. It is also interesting to notice that the damage of cable 939R is best seen through the  $I_S$  degradation rather than through either  $I_c$  or  $RRR$  degradation. For this cable,  $I_S$  is reduced by a factor of 2 or larger in the extracted strands with respect to the round wires, whereas its  $RRR$  is not degraded more, if anything less, than in the other two non-damaged cables shown in figure.

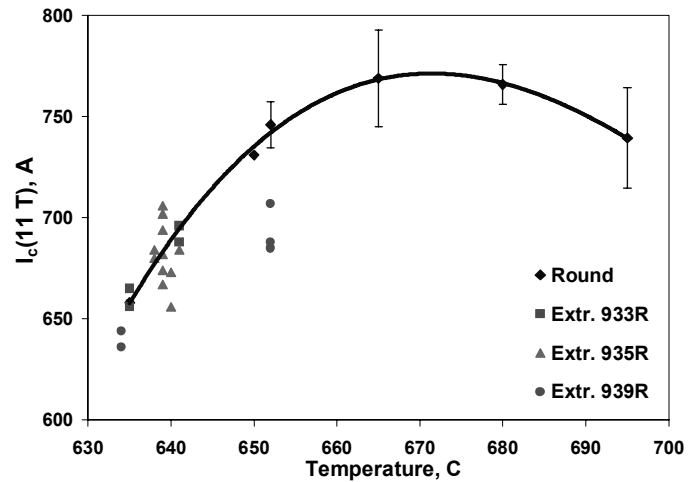


Fig. 6.  $I_c(11 T)$  as measured at 4.2 K at BNL for strands extracted from three different cables as a function of reaction temperature for 48 to 50 h durations. Results are compared against round strand data.

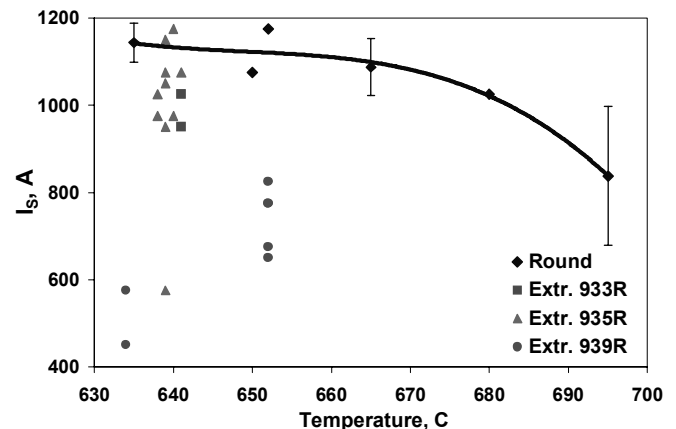


Fig. 7.  $I_S$  as measured at 4.2 K at BNL for strands extracted from three different cables as a function of reaction temperature for 48 to 50 h durations. Results are compared against round strand data.

To verify stability margins, the cables were measured at self-field with a SC transformer equipped with a Rogowski coil to measure the secondary current [9]. Cable test results are in Table IV. All of the cables in Table IV were reacted in the

vicinity of 640 °C. Cable tests are usually well reproducible, and there is a good consistency between the strand  $I_S$  and the cable quench currents.

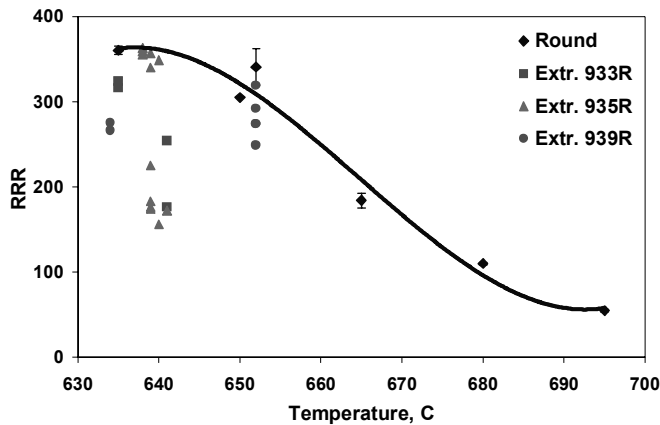


Fig. 8. RRR (averaged over the whole Cu area) as measured at BNL for strands extracted from three different cables as a function of reaction temperature for 48 to 50 h durations. Results are compared against round strand data.

TABLE IV  
CABLE TEST RESULTS

| Cable ID    | Technology | Impregnation | No. quenches | Cable Ave. $I_q$ , kA | Ave. $I_q$ , strand, A | Min. $I_q$ , strand, A | $R_{splice}$ , $n\Omega$ |
|-------------|------------|--------------|--------------|-----------------------|------------------------|------------------------|--------------------------|
| 926R (SQ)   | MJR        | Y            | 12           | 18.4                  | 918                    | 898                    | 2.9                      |
| “           | “          | N            | 13           | 18.9                  | 943                    | 892                    | 4.8                      |
| 928R-B (TQ) | MJR        | Y            | 12           | 19.8                  | 734                    | 697                    | 3.1-3.9                  |
| “           | “          | N            | 16           | 19.7                  | 729                    | 688                    | 2.3                      |
| 928R-B (TQ) | “          | N            | 14           | 20.4                  | 755                    | 732                    | 2.8-3.2                  |
| 932R-A (TQ) | “          | N            | 14           | 23.5                  | 869                    | 851                    | 2.5                      |
| 935R (SR)   | RRP        | Y            | 18           | 18.1                  | 906                    | 807                    | 2.7-2.5                  |
| “           | “          | N            | 16           | 18.7                  | 935                    | 878                    | 2.9-3.1                  |
| 942R (LR)   | “          | N            | 17           | 19.7                  | 987                    | 945                    | 3.0-3.2                  |
| 933R (TQ)   | RRP        | N            | 11           | 22.6                  | 836                    | 762                    | 2.9-3.0                  |
| “           | “          | N            | 15           | 20.1                  | 745                    | 583                    | 3.2-3.4                  |
| 939R (TQ)   | “          | N            | 15           | 19.1                  | 708                    | 666                    | 2.6-2.8                  |
| “           | “          | N            | 16           | 18.7                  | 693                    | 650                    | 4.1-4.4                  |
| 940R (TQ)   | “          | N            | 17           | 21.1                  | 780                    | 721                    | 3.0                      |
| 946R (TQ)   | “          | N            | 9            | 21.9                  | 811                    | 768                    | 2.2-4                    |
| 947R (TQ)   | “          | N            | 13           | 23.3                  | 864                    | 848                    | 1.7                      |

## VII. PREDICTION OF SHORT SAMPLE LIMITS

Witness samples are used to predict short sample limits (SSL) for coils, which are typically tested at 4.5 K. Round and extracted strand as well as cable samples were included as witnesses during reaction of quadrupoles TQS01 and TQC01, and of small racetrack SRS01. The former are made of four double-layer cos-theta coils, whose cable is made of 27 MJR strands. The latter is a small racetrack model to be used as technology transfer from LBNL to BNL. In this case the cable (ID 935R) is made of 20 RRP strands. For an accurate representation of the actual thermal cycles respectively seen by the coils and by the witness samples, type K calibrated thermocouples are placed in various locations.

Given a difference of up to ~9% at 11 T between average  $I_c$  values obtained at BNL and those obtained at FNAL for extracted strands belonging to the same billet, short sample limits were calculated separately from FNAL and BNL data.

Each  $I_c$  vs.  $B$  curve was parameterized using [8], and the critical surfaces for the cable were then obtained at 4.5 K. Billet blend was included in the prediction, the effect of self-field was not. Table IV shows the SSL limit values.

TABLE V  
SHORT SAMPLE LIMIT PREDICTIONS

| Magnet | $I_q$ (FNAL), kA | $I_q$ (BNL), kA | $B_{peak}$ , T | $G$ , T/m | $I_{q, strand}$ , A |
|--------|------------------|-----------------|----------------|-----------|---------------------|
| SRS01  | 9.6              | 9.8             | 12.2-12.4      | -         | 480-490             |
| TQS01  | 12.1             | 12.3            | 11.1-11.3      | 217-220   | 448-455             |
| TQC01  | 12.7             | 12.8            | 10.9-11.1      | 212-215   | 470-478             |

## VIII. SUMMARY

An RRP strand of 0.7 mm diameter is being used as workhorse material in the LARP Magnet R&D program. HT optimization studies showed that whereas the largest  $I_c$ 's are obtained at reaction temperatures between 660 °C and 680 °C, the largest  $I_S$ 's are found below 660 °C. To provide a conservative margin to magnet operation, 640 °C was chosen for LARP coil reaction. Effects of cabling were measured using strands extracted from all the produced cables. It was found that filament damage in a cable is best seen through  $I_S$  degradation rather than either  $I_c$  or RRR degradation. Cable tests at self field are usually in good consistency with strand  $I_S$ . Short sample limit predictions were obtained using witness samples for all fabricated magnets.

Through magnetization measurements, it was found that the  $I_c(1.8 K, 12 T)$  is a factor of 1.35 larger than  $I_c(4.2 K, 12 T)$ . However, at low field flux jumps at 1.8 K are so large that they reduce the magnetization amplitude by about 30% compared to data at 4.2 K. This will be a concern for magnet operation in superfluid He, and prompts once again strand designs with smaller filament sizes.

## ACKNOWLEDGEMENT

The authors wish to thank Lance Cooley for his contribution to the heat treatment studies.

## REFERENCES

- [1] R. Bossert et al., “Development of LARP Technological Quadrupole (TQC) Magnets”, paper 1LK02, this Conference.
- [2] S. Caspi et al., “Fabrication and Test of TQS01 – a 90 mm Nb<sub>3</sub>Sn Quadrupole Magnet for LARP”, paper 4LX03, this Conference.
- [3] P. Wanderer et al., “Design of Nb<sub>3</sub>Sn Coils for LARP Long Magnets”, paper 1LL01, this Conference.
- [4] F. Nobrega et al., “Fabrication and Test of 2-m Long Nb<sub>3</sub>Sn Dipole Mirror Magnet”, paper 1LK08, this Conference.
- [5] E. Barzi et al., “Performance of Nb<sub>3</sub>Sn RRP Strands and Cables Based on a 108/127 Stack Design paper”, paper 4MW06, this Conference.
- [6] E. Barzi et al., “Round and Extracted Nb<sub>3</sub>Sn Strand Tests for LARP Magnet R&D”, IEEE Trans. Appl. Sup., V. 16, No. 2, June 2006, p. 319.
- [7] D. R. Dietderich et al., “Cable R&D for LARP”, this Conference.
- [8] L. T. Summers et al., “A model for the prediction of Nb<sub>3</sub>Sn critical current as a function of field, temperature, strain and radiation damage”, IEEE Trans. Magn., 27 (2): 2041-2044 (1991).
- [9] D. Turroni et al., “Study of Nb<sub>3</sub>Sn Cable Stability at Self-field using a SC Transformer”, IEEE Trans. Appl. Sup., V. 15, No. 2, June 2005, p. 1537.